ARTICLES
https://doi.org/10.1038/s41929-022-00825-z

nature catalysis

Check for updates

Nickel-catalysed asymmetric heteroarylative cyclotelomerization of isoprene

Gong Zhang[1,2], Chao-Yang Zhao[1,2], Xiang-Ting Min[1], Ying Li[1,2], Xiang-Xin Zhang[1,2], Heng Liu[1,2], Ding-Wei Ji[1], Yan-Cheng Hu[1] and Qing-An Chen[1,2] ✉

Monoterpenoids are a class of isoprenoids produced from geranyl diphosphate by various monoterpene synthases. Nature has evolved over millions of years to produce various cyclic monoterpenoids. Herein, we present a serendipitous creation of an unnatural monoterpene skeleton through heteroarylative telomerization of isoprene with heterocycles. Under nickel catalysis, a series of cyclic monoterpene derivatives bearing quaternary carbon stereocentre are constructed with up to 98% yield and 97% enantiomeric excess. Preliminary mechanistic studies suggest this atom-economic reaction proceeds through an enantioselective dimerization of isoprene and a sequential C–H alkylation of heterocycles pathway. This work not only contributes an efficient enantioselective transformation of bulk chemical isoprene, but also provides a guide to create an unnatural monoterpene framework that may exhibit different biological activities.

As the largest and structurally most diverse class of natural products, terpenoids exist in almost all living organisms and function physiologically[1–3]. In nature, the biosynthesis of terpenoids begins with the condensation of isopentenyl diphosphate and dimethylallyl diphosphate to form geranyl diphosphate (GPP) by geranyl pyrophosphate synthase (GPPase). Through a key intermediate (Geranyl cation), monoterpenes and monoterpenoids are produced from GPP under enzymatic catalysis (Fig. 1a)[4–7]. Depending on the specific property of cyclases, cyclic monoterpenes and their derivatives (such as limonene, pinene, camphor, terpineol, carene and menthol) are structurally diverse, which brings different and important applications to academia and industry, such as natural product synthesis, perfumes and pharmaceuticals. Although nature has evolved over millions of years, a seemingly endless number of (enzyme-mediated) carbocation cyclizations lead to seven representative carbocyclic skeletons (Fig. 1a), which are often further oxidized and rearranged to give other monoterpenoids. Therefore, the creation of an additional monoterpene skeleton by an artificial catalytic system is of profound challenge and significance. The achievement of more structural diversity beyond the current skeletons would be good for the discovery of new bioactive candidates for academic research and industry.

As an easily available bulk chemical, isoprene is an attractive precursor for production of terpenes and terpenoids[8–10]. In 1967, Smutny and Takahashi reported a transition metal-catalysed telomerization of 1,3-butadiene with nucleophiles[11–13]. Encouraged by this pioneering work, Beller, Finn, Réau, Navarro and Carbó developed nucleophilic telomerization of isoprene to produce acyclic monoterpenoids (Fig. 1b)[14–22]. Although decent regioselectivities have been achieved, enantioselectivity has never been demonstrated. Beside these issues, nucleophilic cyclotelomerization of isoprene is still unexploited (Fig. 1b).

Heterocyclic compounds, such as purines and imidazoles, play important roles in medicines and natural products. Therefore, tremendous effort has been devoted to the functionalization of these compounds. Among them, the transition metal-catalysed C–H functionalization process represents the most atom- and step-economic protocol[23–25]. Recently, Ellman, Cavell, Ye, Ackermann and Cramer et al. have disclosed direct C–H heteroarylations of simple alkenes under Ni catalysis[26–31]. Encouraged by these precedents and our biomimetic transformations of isoprene[32–36], we imagined developing an asymmetric heteroarylative cyclotelomerization of isoprene (Fig. 1b). To realize this proposal, we had to address the following challenges: First, isoprene is the simplest but hardest unsymmetric diene for regioselective functionalization. The telomerization can theoretically generate up to >60 acyclic isomers and >90 cyclic isomers[37]. These issues make this process a formidable challenge. Second, our previous work indicates that direct hydrofunctionalization of isoprene is a relatively easier process than nucleophilic dimerization. By addressing these challenges, we herein demonstrate an efficient Ni-catalysed asymmetric heteroarylative cyclotelomerization of isoprene (Fig. 1c). The atom-economic protocol generates a series of cyclic monoterpene derivatives bearing a quaternary carbon stereocentre with up to 98% yield and 97% enantiomeric excess (e.e.). It also provides an important complement for the existed natural monoterpenoids in terms of structural framework.

Results

Reaction optimization. Caffeine **1a** and isoprene **2a** were chosen as the model substrates to test our hypothesis (Supplementary Table 1). Initially, a series of ligands were screened under earth abundant nickel catalysis. With low-valent $Ni(COD)_2$ as precatalyst, widely used phosphine ligands, such as PPh_3 and BINAP, were found to be ineffective. In contrast, *N*-heterocyclic carbene ligands (NHC) gave unique reactivity and selectivity[38–40]. When IMes•HCl was used as a ligand precursor, a mixture of mono-prenylated products **4a** and **4b** were obtained in the presence of MeONa (entry 1). The use of EtONa led to **4b** as a main product (entry 2). No product was formed using MeOLi as an additive (entry 3). From the evaluation of alkali metal *tert*-butoxides (entries 4–6), an unexpected heteroarylative telomer **3a** was observed in the presence of ^{t}BuONa (entry 6). When using **L2** as a ligand, the yield of **3a** increased to 81% without the production of **4a** and **4b** (entry 7). When further screening the species of base, caffeine **1a** was converted to telomer **3a** at a 96% yield

[1]Dalian Institute of Chemical Physics, Chinese Academy of Sciences, Dalian, China. [2]University of Chinese Academy of Sciences, Beijing, China. ✉e-mail: qachen@dicp.ac.cn

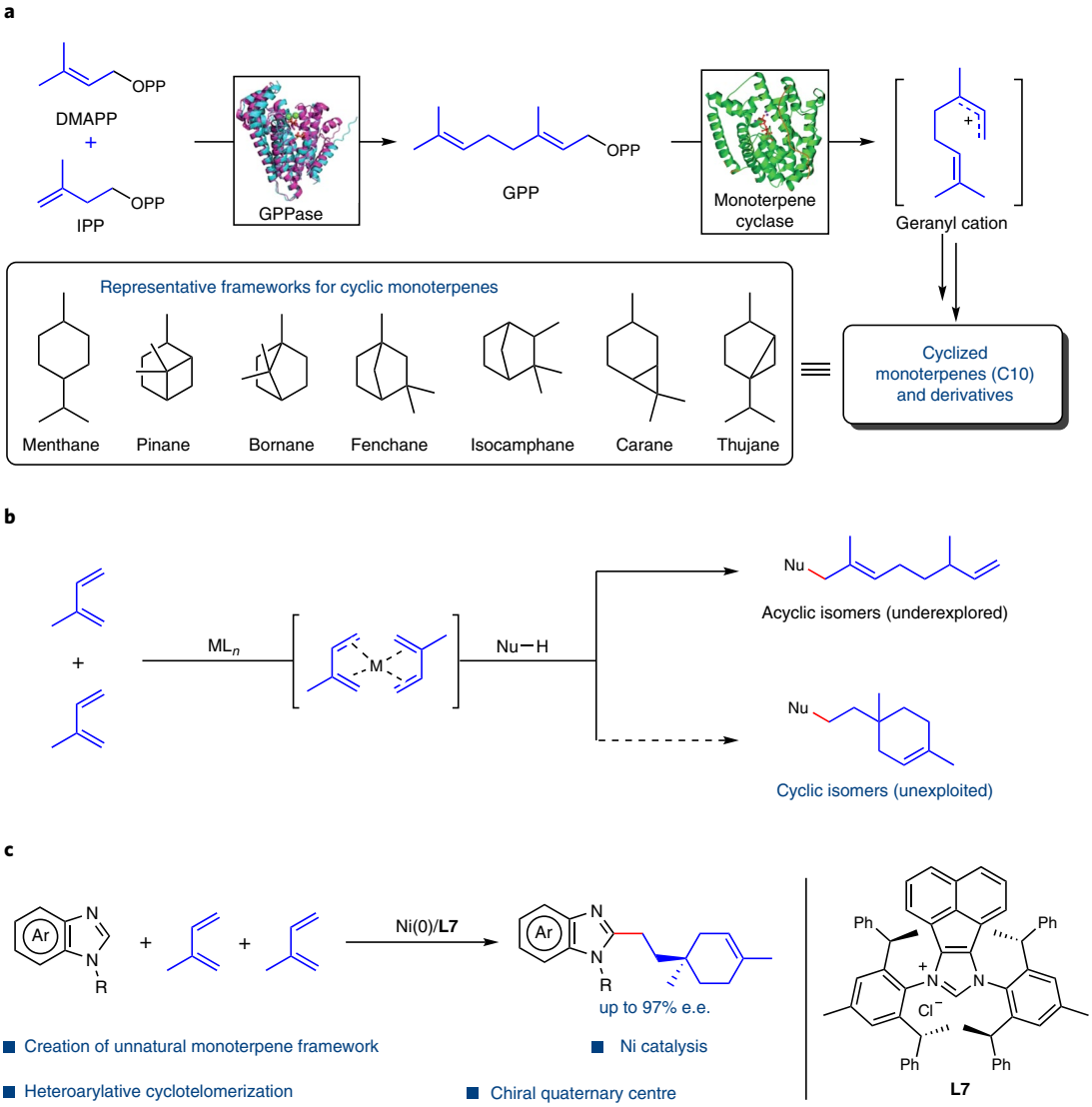

Fig. 1 | Catalytic synthesis of monoterpenoids. a, Synthesis pathway for cyclic monoterpenoides in nature. **b**, State of the art: transition metal-catalysed telomerization of isoprene. **c**, This work: Ni-catalysed asymmetric heteroarylative telomerization of isoprene. DMAPP, dimethylallyl diphosphate; IPP, isopentenyl diphosphate; PP, diphosphate.

with EtONa as a base (entry 8). Decreasing the amount of EtONa to 50 mol%, the yield was reduced to 84% (entry 9). Saturated NHC ligand **L3** could also facilitate the formation of telomer **3a** (entry 10). Given that **3a** possesses a chiral quaternary centre, further studies were carried out to induce the enantioselectivity. No desired product was detected using chiral ligand **L4** bearing a free hydroxyl group (entry 11). To our delight, sterically hindered C2-symmetric NHC ligand **L5** provided the telomer **3a** in 97% yield and 80% e.e. (entry 12). A comparable result was achieved in the presence of **L6** (entries 13). More structurally rigid NHC ligand **L7** gave **3a** in a higher enantioselectivity (93% e.e., entry 14). Desired product **3a** was delivered in 88% yield and 93% e.e. using ^{t}BuONa (entry 15). No improvement in enantioselectivity was observed by decreasing the reaction temperature (entry 16).

Substrate scope. With the optimized conditions in hand, we sought to examine the scope of this telomerization reaction (Fig. 2). In general, for caffeine analogues **1a**–**1d**, the reactions proceeded well under the standard conditions, affording the products **3a**–**3d** in 73–96% yield with 93–94% e.e. Substrate **1e** derived from etofylline was also amenable to the procedure, and telomer **3e** was furnished in 87% yield and 94% e.e. The N^7-acetal substituent was also tolerated in this protocol, giving rise to **3f** in a high yield and enantioselectivity. When N^7-prenyl theophylline was involved in this reaction, deprenylated product **3h** was afforded as the main product along with a small amount of **3g**. The introduction of a coordinative pyridyl group was accommodated to provide **3i** at a 90% yield and 93% e.e. Also, N^7-benzyl theophylline participated well in this asymmetric telomerization reaction (**3j**). A broad range of the substituents including benzyl, isobutyl, cyclopropylmethyl and 5-oxohexyl on N^1 atom were all compatible with the process (**3k**–**3n**). When the methyl groups of caffeine were replaced with benzyl substituent, the target telomer **3o** was obtained at a 96% yield and 93% e.e. Notably, the cyclogeranylation of caffeine still took place smoothly on a gram-scale even with a lower catalyst loading (2.5 mol%), and **3a** was delivered in 93% yield without a loss of enantioselectivity. The absolute configuration of **3a** was unambiguously determined by X-ray analysis (CCDC 2127531).

Adenine acts as a nucleobase in both the nucleic acids DNA and RNA. This protocol could be further extended to the asymmetric

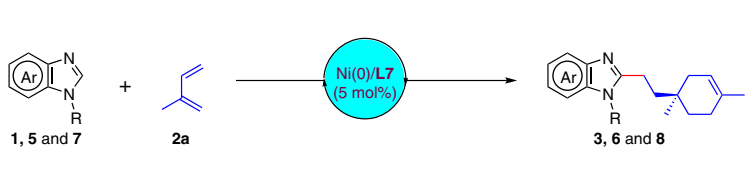

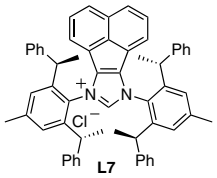

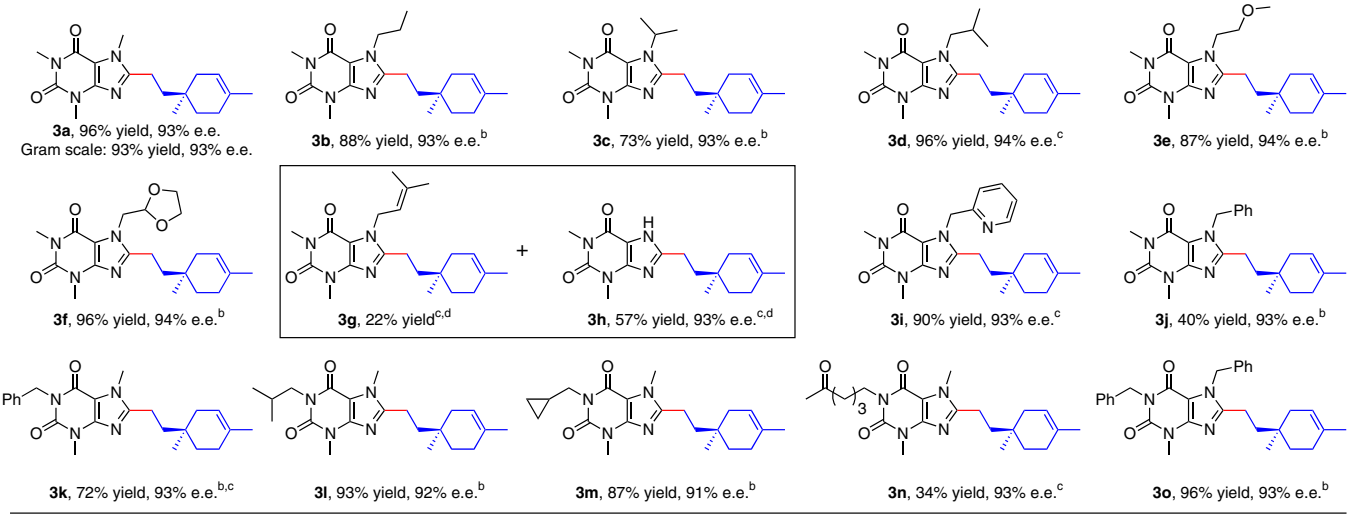

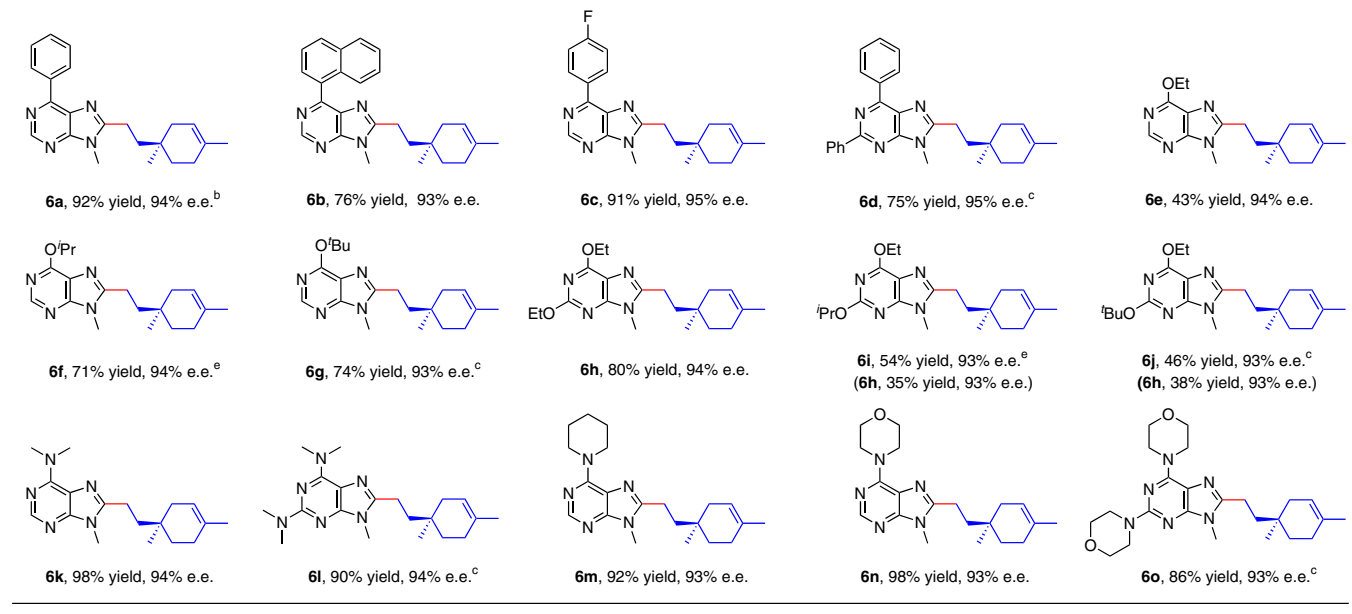

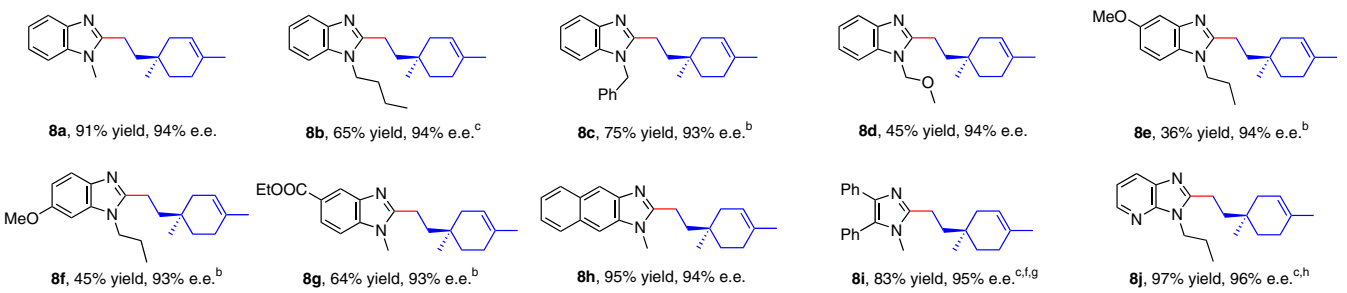

Fig. 2 | Substrate scope of purines, adenines and imidazoles. [a]Conditions: **1**, **5** or **7** (0.20 mmol), **2a** (0.80 mmol), $Ni(COD)_2$ (5 mol%), **L7** (5 mol%), EtONa (100 mol%) and toluene (1.0 ml) at 100 °C. In all cases, an isolated yield is given and e.e. was determined by chiral HPLC. [b]Solvent is toluene:NMP (V/V = 1.0:0.1). [c]*t*-BuONa (100 mol%). [d]Solvent is toluene/benzotrifluoride (V/V = 1.0:0.1). [e]*i*-PrONa (100 mol%). [f]Solvent is hexane. [g]120 °C. [h]$FeCl_3$ (50 mol%). NMP, *N*-methyl pyrrolidone.

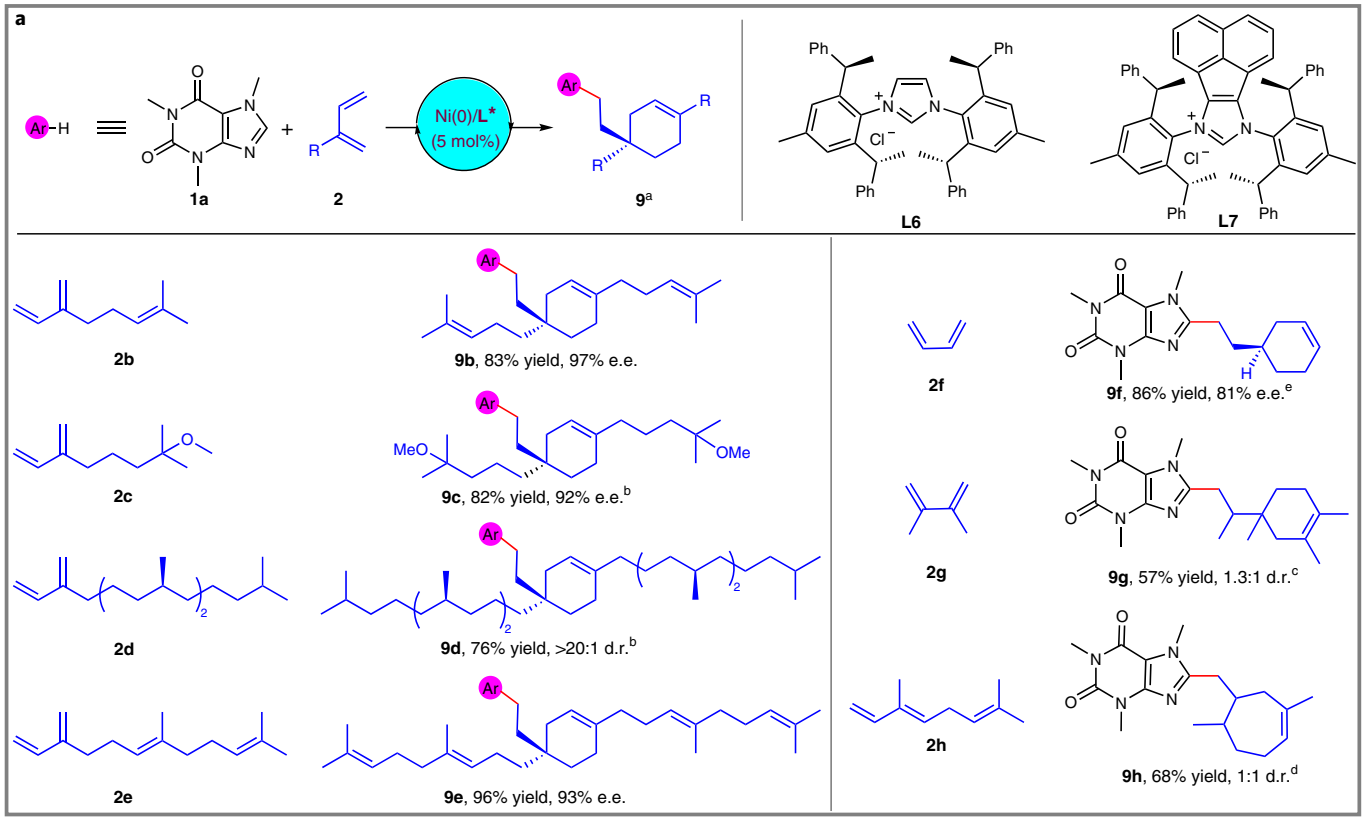

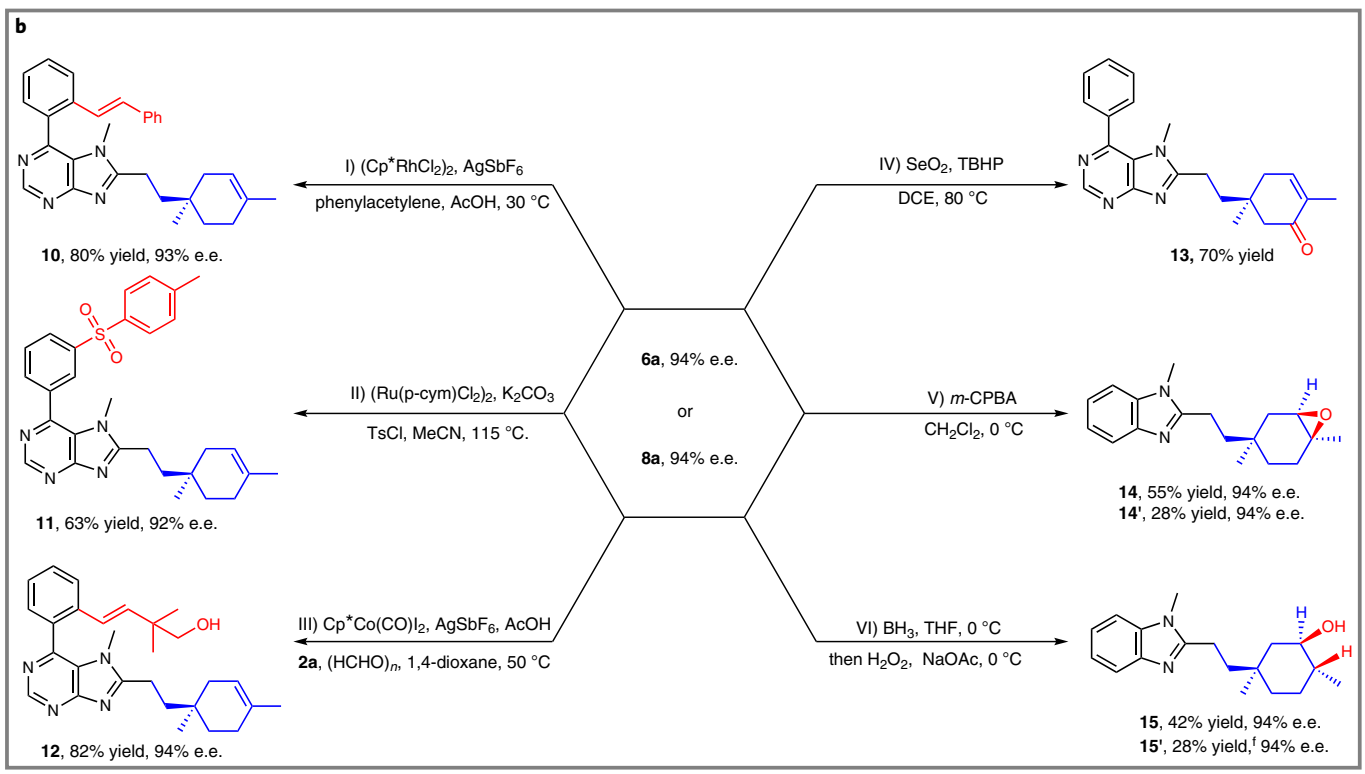

Fig. 3 | Substrate scope of other conjugated dienes and transformation of chiral telomers. a, The scope of dienes. **b**, The transformations of chiral telomers **6a** and **8a**. [a]Conditions: **1a** (0.20 mmol), **2** (0.80 mmol), $Ni(COD)_2$ (5 mol%), **L7** (5 mol%), [t]BuONa (100 mol%), hexane (1.0 ml), 100 °C. In all cases, an isolated yield is given and e.e. was determined by chiral HPLC. [b]Toluene was used. [c]Toluene:1,4-dioxane (1.0:0.1) was used. [d]THF was used. [e]Toluene and **L6** were used. [f]**15′** is a mixture of regioisomers, ratio is 2:1.

modification of adenine derivatives. For instance, a variety of 6-aryl substituted adenines were all applicable to this transformation, affording the corresponding products (**6a**–**6c**) in 76–92% yield and 93–95% e.e. The coupling between 2,6-diphenyl adenine with isoprene led to the formation of **6d** in 75% yield and 95% e.e. Those adenines possessing diverse alkoxyl substituents, including ethoxyl,

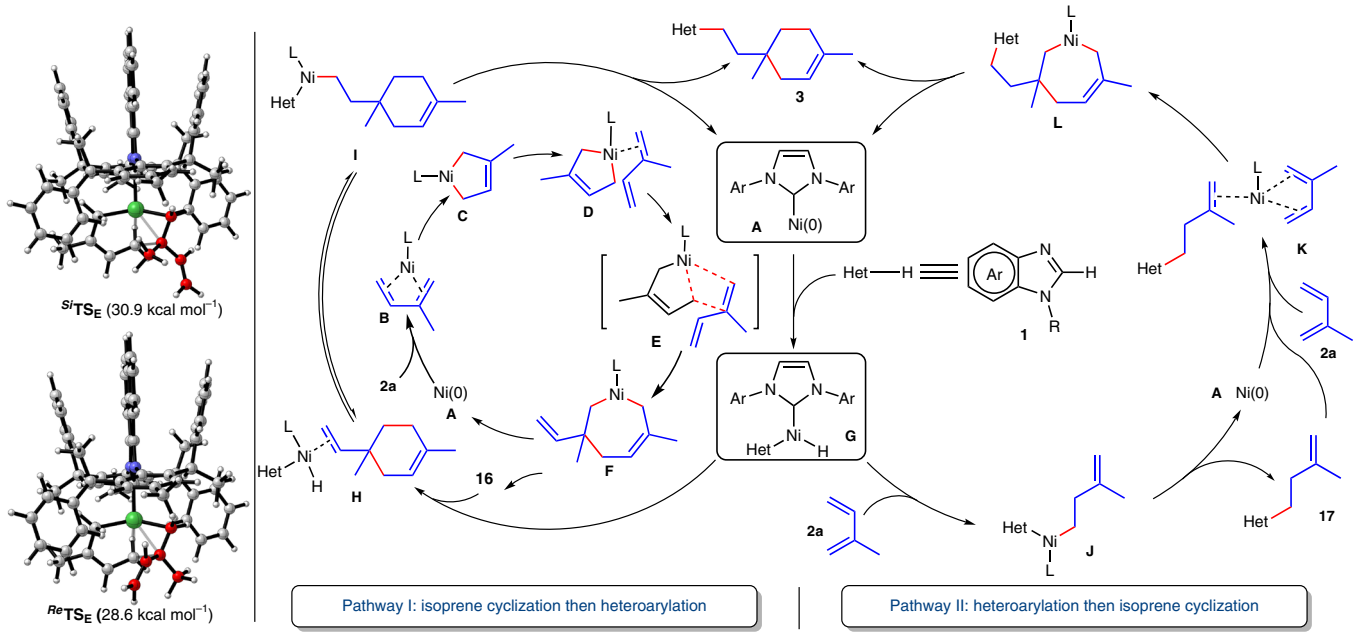

Fig. 4 | Proposed mechanism and calculated transition states. The geometry optimizations performed by density functional theory calculations at the SMD(toluene)-M06/(SDD(Ni)/6-311+G(d,p))//M06/(LANL2DZ(Ni)/6-31G(d)) level.

tert-butoxyl and isopropoxyl, were suitable substrates as well, providing the desired products with good to excellent e.e. values and yields (**6e**–**6g**). Both cyclogeranylations of 2-O^{i}Pr and 2-O^{t}Bu adenines delivered **6h** as the main product under the optimized conditions, probably due to the facile alkoxyl exchange with EtONa. Accordingly, in these cases, ^{i}PrONa and ^{t}BuONa were selected as the optimal bases, respectively, and the target products **6i** and **6j** were obtained in decent yields. Moreover, a set of nitrogen-containing substituents, such as dimethylamino, piperidyl and morpholinyl, were also well tolerated (**6k**–**6o**).

Benzimidazole is a fundamental class of nitrogen-containing heterocycles that are present in many clinically useful drugs, due to their potent biological and medicinal activities. The cyclogeranylation of benzimidazoles also worked well under this nickel catalysis. *N*-Me, –^{n}Bu, –Bn, –MOM (methoxymethyl ether) substituted benzimidazoles were converted into their corresponding products **8a**–**8d** at a 45–91% yield and 93–94% e.e. The properties of substituents on the phenyl ring exerted minimal influence on the outcome. Both electron-donating and -withdrawing groups (**7e**–**7g**) could be successfully applied in this transformation. Naphthoimidazole and isoprene underwent this coupling efficiently, producing **8h** at a 95% yield and 94% e.e. In addition, imidazole was compatible with the process, resulting in **8i** at a 83% yield and 95% e.e., although its C–H bond is more inert than that of benzimidazole. The cyclogeranylation of biologically important imidazopyridine **7j** took place as well, generating **8j** at a 97% yield and 96% e.e.

Next, the substrate scope regarding terpenes was further explored with caffeine (**1a**) as a model substrate (Fig. 3). Terpenes bearing two isoprene units, such as myrcene (**2b**) and its derivatives (**2c**) proceeded smoothly to deliver the telomer products (**9b**, **9c**) in high yields (82–83%) and excellent enantioselectivities (92–97%). Phytadiene (**2d**), derived from chlorophyll, was a suitable coupling partner and the expected product **9d** was formed at a 76% yield and >20:1 d.r. (diastereomeric ratio) Sesquiterpene farnesene **2e** reacted with caffeine smoothly, resulting in **9e** at a 96% yield and 93% e.e. Also, simple butadiene **2f** and 2,3-dimethyl-1,3-butadiene **2g** were applicable to the protocol, albeit with slightly decreased selectivities. When ocimene, an isomer of myrcene **2b**, was used as the partner, the reaction did not deliver product **9b**, while **9h** was isolated at a 68% yield and 1:1 d.r.

To demonstrate the practical use of this protocol, further synthetic transformations of chiral telomers **6a** and **8a** were carried out (Fig. 3). By taking advantage of the inherent directing ability of adenine, C–H alkenylation of **6a** with phenylacetylene occurred with a high efficiency under Rh(III) catalysis[41], providing **10** at a 80% yield and 93% e.e. With [Ru(*p*-cym)Cl$_2$]$_2$ as the catalyst[42], the coupling between **6a** and tosyl chloride resulted in the formation of *meta*-sulfonylated product **11** at a 63% yield and 92% e.e. Next, following our previously developed strategy[33], Cp*Co(CO)I$_2$-catalysed three-component reaction of **6a**, isoprene with paraformaldehyde gave rise to **12** at a 82% yield and 94% e.e. In addition, in the presence of SeO$_2$ and TBHP (*tert*-butyl hydroperoxide), the allylic position of cyclogeranyl motif could undergo selective oxidation to furnish *α*,*β*-unsaturated ketone **13** at a 70% yield. In the presence of *m*-CPBA, chiral telomer **8a** was transformed into the useful epoxide **14** and its diastereomer **14′** both with 94% e.e. Moreover, the product **8a** underwent hydroboration–oxidation to afford alcohol **15** with 94% e.e. The configurations of **14** and **15** were determined using nuclear Overhauser effect spectroscopy.

Mechanistic studies. Isoprene cyclization and C–H alkylation of heterocycle are two features of this asymmetric heteroarylative cyclotelomerization, but which process occurs first? On the basis of our observations and previous reports[20,22], two plausible mechanisms for Ni-catalysed asymmetric heteroarylative cyclotelomerization are proposed in Fig. 4. First of all, before the on-cycle catalytic reaction, Ni^{0}(NHC) **A** is formed in situ by the reaction between Ni(COD)$_2$, chiral NHC **L7** and base. For the pathway **I**, the dimerization of isoprene proceeds before C–H alkylation of heterocycle. In situ generated Ni^{0}(NHC) species coordinates with one molecule isoprene to form the complex **B**, which undergoes oxidative cyclometallation to give a five-membered nickelacycle **C**. Through the coordination with another isoprene, complex **D** proceeds with a migratory insertion to furnish a seven-member nickelacycle **F** via a transition state **E**. With the formation of new C–C bond, reductive elimination of Ni(II) species **F** yields the desired dimerization

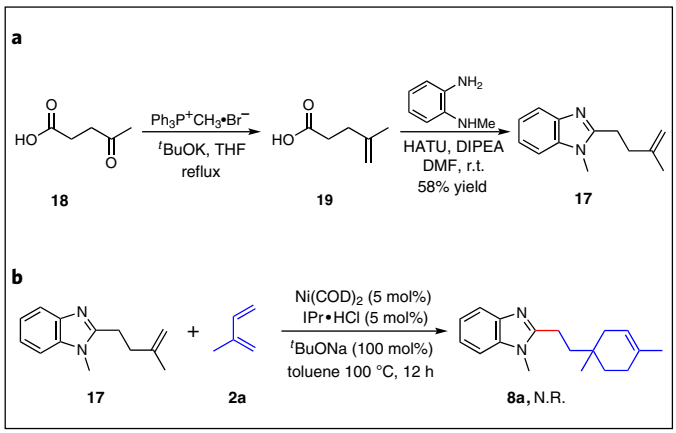

c

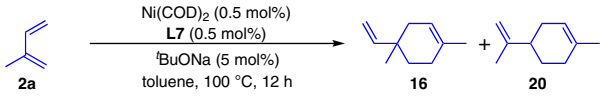

Entry	Deviation from standard conditions	Yield of **16**	Yield of **20**
1	None	36%	12%
2	Using IPr instead of **L7** without ^{t}BuONa	22%	19%
3	Without $Ni(COD)_2$ and **L7**	<1%	1%
4	Without **L7**	<1%	3%

d

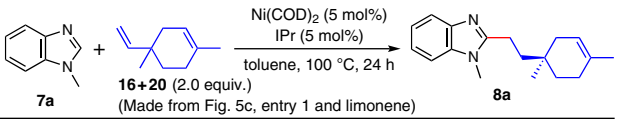

Entry	**16**/**20**	^{t}BuONa (mol%)	Yield of **8a**	e.e. of **8a**
1	3:1	0	67%	92%
2	1:1	0	16%	92%
3	1:3	0	ND	–
4	3:1	10	98%	92%
5	1:1	10	81%	93%
6	1:3	10	73%	93%
7	1:10	10	ND	–

e

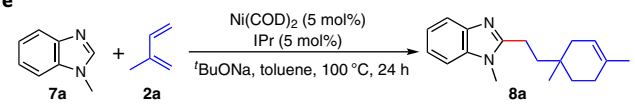

Entry	^{t}BuONa (mol%)	Yield of **8a**
1	100	87%
2	10	57%
3	0	ND

f

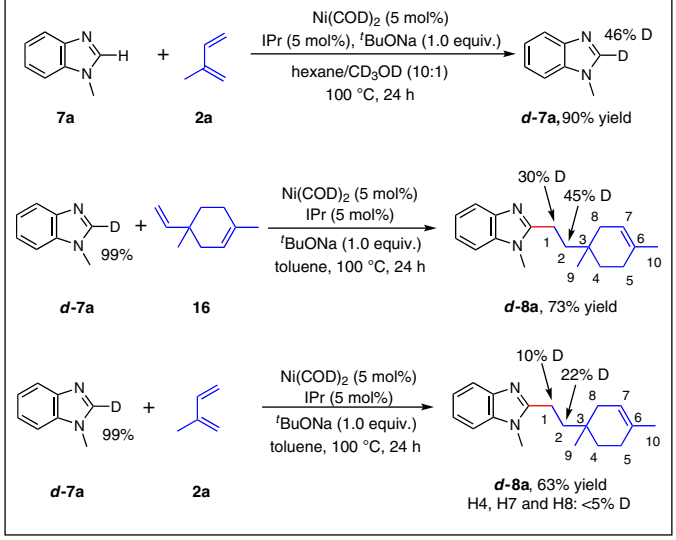

g

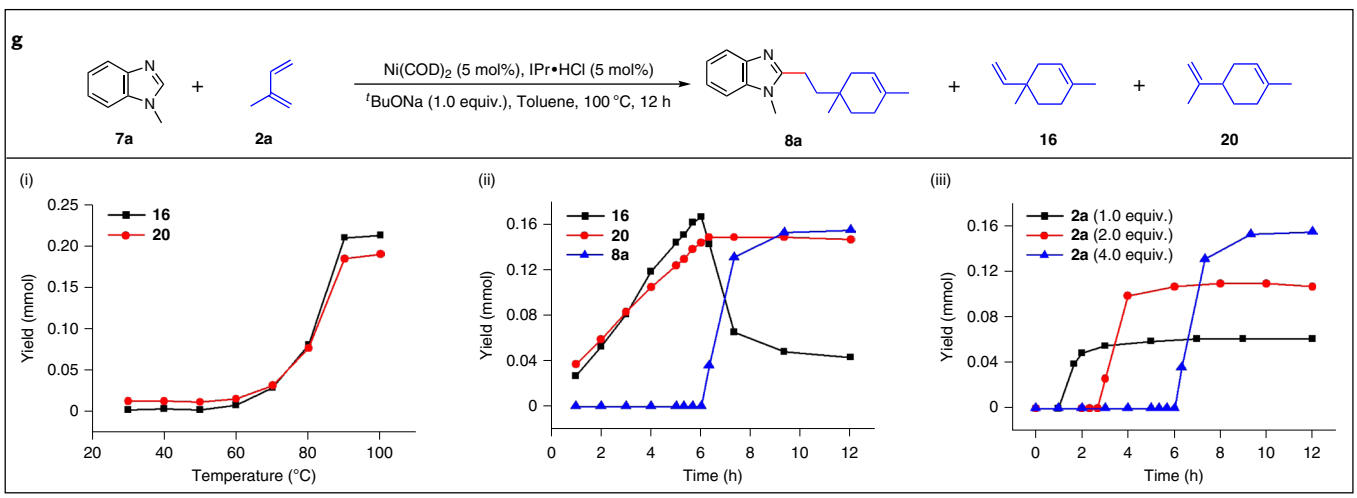

Fig. 5 | Mechanistic studies. a, The synthesis of hydroheteroarylation intermediate **17**. **b**, Cyclization of hydroheteroarylation intermediate. **c**, Direct dimerization of isoprene. **d**, The effect of base and limonene **20** on functionalization of **7a**. **e**, The effect of base on the heteroarylative cyclotelomerization of isoprene. **f**, Deuterium labelling experiments. **g**, Kinetic studies for the heteroarylative cyclotelomerization of isoprene. (i) Temperature effect on the formation of **16**/**20** without **7a**. (ii) Kinetic profile under the standard condition. (iii) The concentration effect of **2a** on the induction period. r.t., room temperature; N.R., no reaction.

product **16**. Meanwhile, nickel-hydride **G** is generated through a C–H bond activation between **A** and heterocycle substrates. Later, the resulting dimer **16** coordinated with Ni–H **G** to form complex **H**, which undergoes migratory insertion and reductive elimination to afford desired product **3** and regenerate the nickel catalyst. For the pathway **II**, the C–H alkylation of heterocycles proceeds before the cyclization. The coordination of Ni–H **G** with one isoprene facilitates the migratory insertion to afford Ni(II) complex **J**.

A subsequent reductive elimination yields mono-isoprenyl product **17**. Next, the regenerated Ni(0) species **A** undergoes oxidative cyclometallation with **2a** and **17** to form desired seven-membered nickelacycle **L**. Finally, reductive elimination of intermediate **L** results in desired heteroarylative cyclotelomerization product **3** and regenerates the nickel catalyst for next catalytic cycle.

To differentiate these two proposed mechanisms, some control experiments were designed and carried out (Fig. 5). Although being a proposed intermediate for pathway **II**, mono-isoprenyl product **17** could not be detected through monitoring the reaction. To further exclude the possibility of pathway **II**, mono-isoprenyl product **17** was prepared through a condensation reaction between **19** and N^1-methylbenzene-1,2-diamine (Fig. 5a). The control coupling reaction between **17** and isoprene **2a** gave no desired product **8a** (Fig. 5b). This result indicates that C–H alkylation of heterocycles does not proceed before the cyclization (Fig. 4, pathway **II**). Therefore, the detection of the assumed dimer **16** in pathway **I** became the preferential target. Accompanied by the formation limonene **20**, 36% yield of desired dimer **16** was obtained under Ni catalysis in the absence of heterocycle substrate (Fig. 5c, entry 1). The use of achiral NHC ligand IPr gave a similar result but lower selectivity (Fig. 5c, entry 2). Only trace amounts of **16** or **20** were observed from the control experiments (Fig. 5c, entrie 3 and 4). These results (Fig. 5c, entries 1 versus 3 and 4) indicate that desired dimer **16** and limonene **20** are catalyst-induced products. The e.e. of dimer **16** could not be determined directly by various chiral gas chromatography or high-performance liquid chromatography (HPLC) columns.

Subsequently, the coupling of the dimer mixture (Fig. 5c, entry 1) with **7a** afforded the desired product **8a** in 92% e.e. in the presence of achiral NHC ligand IPr (Fig. 5d, entry 1). These results indicate that the dimerization of isoprene for the formation **16** is the enantioselective determining step. A higher yield but the same enantioselectivity (92% e.e.) was obtained for **8a** by increasing the using of base additive to 10 mol% (Fig. 5d, entry 4). To probe the importance of the base and its role, several more control experiments have been conducted. By increasing the concentration of limonene **20**, the yield of **8a** decreased notably in the absence of ^{t}BuONa (Fig. 5d, entries 1–3). The addition of 10 mol% ^{t}BuONa dramatically improved the yield of **8a** when the concentration of limonene **20** was not too high (Fig. 5d, entries 4–6 versus 1–3). When the ratio **20:16** was increased to 10:1, no desired product was observed even in the presence of 10 mol% ^{t}BuONa. These results indicate the existence of some catalyst deactivation in the presence of high concentration of limonene **20**. It also suggests that a base is not required for the 4+2 cycloaddition or subsequent C–H bond activation. However, the addition of base helps the reactivation of catalyst resting species for the desired catalytic cycle (Supplementary Fig. 5). A similar base effect was observed in the direct heteroarylative cyclotelomerization of isoprene **2a** with imidazole **7a** (Fig. 5e, entries 1–3).

What is more, subjecting substrate **7a** to the optimized reaction conditions in the presence of CD_3OD revealed a notable H/D scrambling with 46% deuterium incorporation at the C2 position. In addition, deuterium labelling experiments were carried out with **d-7a**. When dimer **16** was used in this reaction, the corresponding product **8a** was obtained with 30 and 45% of deuterium at the H1 and H2 position. The obvious deuterium scrambling may be attributed to the reversible migratory insertion of Ni^{II}-hydride into dimer **16**. When isoprene **2a** was used, deuterium labelling in product **8a** was detected at the H1, H2, H7 and H8 position. The lower deuterium incorporation indicated that migratory insertion of isoprene into Ni^{II}-hydride occurred reversibly (Fig. 5f).

The kinetic studies were carried out further to interpret the reaction process. As shown in Fig. 5g, there is a notable temperature effect on the reactivity for the dimerization of isoprene in the absence of **7a** (Fig. 5g(i)). In the presence of **7a**, the dimer products **16** and **20** were quickly formed at the early stage of the reaction and reached the peak around 6 h. After 6 h, intermediate **16** decreased gradually, whereas the yield of **20** remained constant. The desired product **8a** was not detected at the initial 6 h and then gradually increased with the decrease of **16** (Fig. 5g(ii)). This interesting catalytic induction period brought us to investigate the quantity effect of isoprene. The induction period decreased (from 6 to 1 h) with a decrease in the loading of isoprene **2a** (from 4.0 to 1.0 equiv., Fig. 5g(iii)). These results not only indicate the C–H alkylation of heterocycles will not occur until the dimerization of isoprene is complete, but also suggest that the rate-determining step is isoprene dimerization rather than hydroheteroarylation of dimer **16**. Theoretical calculations indicate that transition state $^{Re}\mathbf{TS}_E$ (leading to the *R*-product, ***R*-16**) is favoured by 2.3 kcal mol^{-1} compared with transition state $^{Si}\mathbf{TS}_E$ (leading to the *S*-product, ***S*-16**) (Supplementary Fig. 6). This is in agreement with the experimentally observed high enantioselectivity favouring the formation of the *R*-product (***R*-16**), which evolves into ***S*-3a**. Thanks to the accumulated benefit from steric hindrance of bulky NHC ligand **L7**, this protocol favours the heteroarylative cyclotelomerization rather than mono-prenylation (Supplementary Fig. 4). Overall, these results hint at the intermediacy of dimer **16** and support that the dimerization of isoprene should proceed before the C–H bond activation (Fig. 5g(iii)).

Conclusions

In conclusion, an unnatural monoterpene skeleton was created in excellent enantioselectivity by a nickel based catalytic system that performs the cascade isoprene dimerization/C–H functionalization. The use of bulky C2-symmetric NHC as a chiral ligand enables the nickel catalysis to tackle the challenges in simultaneous control of the chemo-, regio- and enantioselectivity in this protocol. Various heteroaromatic compounds, such as purine and imidazole analogues were all tolerated well. This chemistry capitalizes on the tandem catalysis mechanism, in which the enantioselective dimerization of isoprene precedes the C–H bond functionalization. It is expected that this protocol may be of broad interest to practitioners pursuing the transformation for terpenes and constitutes a practical alternative to synthesis of natural products and pharmaceuticals.

Methods

General information. Commercially available reagents were used without further purification. Solvents were treated before use according to the standard methods. Unless otherwise stated, all reactions were conducted under an inert atmosphere using standard Schlenk techniques or in a nitrogen-filled glove box. ^{1}H nuclear magnetic resonance (NMR) and ^{13}C NMR and ^{19}F NMR spectra were recorded at room temperature in $CDCl_3$ on a 400 or 700 MHz instrument with tetramethylsilane as the internal standard. Flash column chromatography was performed on silica gel (200–300 mesh). All reactions were monitored by thin-layer chromatography or NMR analysis. High-resolution mass spectrometry data were obtained with a Micromass HPLC-quadrupole-time-of-flight mass spectrometer (electrospray ionization) or Agilent 6540 Accurate-MS spectrometer (quadrupole-time-of-flight).

General procedure for the synthesis of chiral telomers. In a glove box, a sealed tube was charged with **1** (1.0 equiv.), diene (4.0 equiv.), $Ni(COD)_2$ (5 mol%), **L7** (5 mol%), base (1.0 equiv.) and anhydrous toluene (1.0 ml). The reaction tube was sealed with a teflon screw cap, removed from the glove box. Then, the reaction mixture was stirred at 100 °C for 24 h (Figs. 2 and 3). On completion, the mixture was filtered through a short pad of celite, concentrated in vacuo and purified by silica chromatography to afford the products. The enantioselectivity was determined by chiral HPLC.

Data availability

Data relating to the characterization data of materials and products, general methods, optimization studies, experimental procedures, mechanistic studies, mass spectrometry, high-performance liquid chromatography, NMR spectra and computational studies are available in the Supplementary Information. Crystallographic data for the structures reported in this article have been deposited at the Cambridge Crystallographic Data Centre, under deposition numbers CCDC 2127531 (**3a**). Copies of the data can be obtained free of charge via https://www.ccdc.cam.ac.uk/structures/.

Received: 6 January 2022; Accepted: 12 July 2022;
Published online: 18 August 2022

References

1. Oldfield, E. & Lin, F. Y. Terpene biosynthesis: modularity rules. *Angew. Chem. Int. Ed.* **51**, 1124–1137 (2012).
2. Brill, Z. G., Condakes, M. L., Ting, C. P. & Maimone, T. J. Navigating the chiral pool in the total synthesis of complex terpene natural products. *Chem. Rev.* **117**, 11753–11795 (2017).
3. Tu, H.-F., Zhang, X., Zheng, C., Zhu, M. & You, S.-L. Enantioselective dearomative prenylation of indole derivatives. *Nat. Catal.* **1**, 601–608 (2018).
4. Sacchettini, J. C. & Poulter, C. D. Creating isoprenoid diversity. *Science* **277**, 1788–1789 (1997).
5. Hyatt, D. C. et al. Structure of limonene synthase, a simple model for terpenoid cyclase catalysis. *Proc. Natl Acad. Sci. USA* **104**, 5360–5365 (2007).
6. Gao, Y., Honzatko, R. B. & Peters, R. J. Terpenoid synthase structures: a so far incomplete view of complex catalysis. *Nat. Prod. Rep.* **29**, 1153–1175 (2012).
7. Chang, W. C., Song, H., Liu, H. W. & Liu, P. Current development in isoprenoid precursor biosynthesis and regulation. *Curr. Opin. Chem. Biol.* **17**, 571–579 (2013).
8. Nishimura, T., Ebe, Y. & Hayashi, T. Iridium-catalyzed [3 + 2] annulation of cyclic N-sulfonyl ketimines with 1,3-dienes via C-H activation. *J. Am. Chem. Soc.* **135**, 2092–2095 (2013).
9. Nishimura, T., Nagamoto, M., Ebe, Y. & Hayashi, T. Enantioselective [3 . 2] annulation via C-H activation between cyclic N-acyl ketimines and 1,3-dienes catalyzed by iridium/chiral diene complexes. *Chem. Sci* **4**, 4499–4504 (2013).
10. Perry, G. J. P., Jia, T. & Procter, D. J. Copper-catalyzed functionalization of 1,3-dienes: hydrofunctionalization, borofunctionalization, and difunctionalization. *ACS Catal.* **10**, 1485–1499 (2019).
11. Smutny, E. J. Oligomerization and dimerization of butadiene under homogeneous catalysis. Reaction with nucleophiles and the synthesis of 1,3,7-octatriene. *J. Am. Chem. Soc.* **89**, 6793–679 (1967).
12. Takahashi, S., Shibano, T. & Hagihara, N. The dimerization of butadiene by palladium complex catalysts. *Tetrahedron Lett.* **8**, 2451–2453 (1967).
13. Faßbach, T. A., Vorholt, A. J. & Leitner, W. The telomerization of 1,3-dienes - a reaction grows up. *Chem. Cat. Chem.* **11**, 1153–1166 (2019).
14. Keim, W. & Roper, M. Terpene amine synthesis via palladium-catalyzed isoprene telomerization with ammonia. *J. Org. Chem.* **46**, 3702–3707 (1981).
15. Hidai, M. et al. Palladium-catalyzed asymmetric telomerization of isoprene - preparation of optically-active citronellol. *J. Organomet. Chem.* **232**, 89–98 (1982).
16. Keim, W., Kurtz, K.-R. & Röper, M. Palladium catalyzed telomerization of isoprene with secondary amines and conversion of the resulting terpene amines to terpenols. *J. Mol. Catal.* **20**, 129–138 (1983).
17. Maddock, S. M. & Finn, M. G. Palladium-catalyzed head-to-head telomerization of isoprene with amines. *Organometallics* **19**, 2684–2689 (2000).
18. Leca, F. & Reau, R. 2-Pyridyl-2-phospholenes: new P,N ligands for the palladium-catalyzed isoprene telomerization. *J. Catal.* **238**, 425–429 (2006).
19. Jackstell, R., Grotevendt, A., Michalik, D., El Firdoussi, L. & Beller, M. Telomerization and dimerization of isoprene by in situ generated palladium-carbene catalysts. *J. Organomet. Chem.* **692**, 4737–4744 (2007).
20. Gordillo, A., Pachón, L. D., de Jesus, E. & Rothenberg, G. Palladium-catalysed telomerisation of isoprene with glycerol and polyethylene glycol: a facile route to new terpene derivatives. *Adv. Synth. Catal.* **351**, 325–330 (2009).
21. Maluenda, I. et al. Room temperature, solventless telomerization of isoprene with alcohols using (*N*-heterocyclic carbene)-palladium catalysts. *Catal. Sci. Technol.* **5**, 1447–1451 (2015).
22. Colavida, J. et al. Regioselectivity control in Pd-catalyzed telomerization of isoprene enabled by solvent and ligand selection. *ACS Catal.* **10**, 11458–11465 (2020).
23. Ackermann, L., Vicente, R. & Kapdi, A. R. Transition-metal-catalyzed direct arylation of (hetero)arenes by C-H bond cleavage. *Angew. Chem. Int. Ed.* **48**, 9792–9826 (2009).
24. Hartwig, J. F. Regioselectivity of the borylation of alkanes and arenes. *Chem. Soc. Rev.* **40**, 1992–2002 (2011).
25. Gandeepan, P. et al. 3d Transition metals for C-H activation. *Chem. Rev.* **119**, 2192–2452 (2019).
26. Clement, N. D. & Cavell, K. J. Transition-metal-catalyzed reactions involving imidazolium salt/N-heterocyclic carbene couples as substrates. *Angew. Chem. Int. Ed.* **43**, 3845–3847 (2004).
27. Nakao, Y., Kashihara, N., Kanyiva, K. S. & Hiyama, T. Nickel-catalyzed hydroheteroarylation of vinylarenes. *Angew. Chem. Int. Ed.* **49**, 4451–4454 (2010).
28. Shih, W. C. et al. The regioselective switch for amino-NHC mediated C-H activation of benzimidazole via Ni-Al synergistic catalysis. *Org. Lett.* **14**, 2046–2049 (2012).
29. Wang, Y. X. et al. Enantioselective Ni-Al bimetallic catalyzed exo-selective C-H cyclization of imidazoles with alkenes. *J. Am. Chem. Soc.* **140**, 5360–5364 (2018).
30. Diesel, J., Grosheva, D., Kodama, S. & Cramer, N. A bulky chiral N-heterocyclic carbene nickel catalyst enables enantioselective C-H functionalizations of indoles and pyrroles. *Angew. Chem. Int. Ed.* **58**, 11044–11048 (2019).
31. Loup, J., Muller, V., Ghorai, D. & Ackermann, L. Enantioselective aluminum-free alkene hydroarylations through C-H activation by a chiral nickel/JoSPOphos manifold. *Angew. Chem. Int. Ed.* **58**, 1749–1753 (2019).
32. Hu, Y. C., Ji, D. W., Zhao, C. Y., Zheng, H. & Chen, Q. A. Catalytic prenylation and reverse prenylation of indoles with isoprene: regioselectivity manipulation through choice of metal hydride. *Angew. Chem. Int. Ed.* **58**, 5438–5442 (2019).
33. Yang, J. et al. Cobalt-catalyzed hydroxymethylarylation of terpenes with formaldehyde and arenes. *Chem. Sci.* **10**, 9560–9564 (2019).
34. Kuai, C. S. et al. Ligand-regulated regiodivergent hydrosilylation of isoprene under iron catalysis. *Angew. Chem. Int. Ed.* **59**, 19115–19120 (2020).
35. Li, Y. et al. Acid-catalyzed chemoselective C- and O- prenylation of cyclic 1,3-diketones. *Chin. J. Catal.* **41**, 1401–1409 (2020).
36. Jiang, W. S. et al. Orthogonal regulation of nucleophilic and electrophilic sites in Pd-catalyzed regiodivergent couplings between indazoles and isoprene. *Angew. Chem. Int. Ed.* **60**, 8321–8328 (2021).
37. Zhao, C. Y. et al. Bioinspired and ligand-regulated unnatural prenylation and geranylation of oxindoles with isoprene under Pd catalysis. *Angew. Chem. Int. Ed.* **61**, e202207202 (2022).
38. Janssen-Muller, D., Schlepphorst, C. & Glorius, F. Privileged chiral N-heterocyclic carbene ligands for asymmetric transition-metal catalysis. *Chem. Soc. Rev.* **46**, 4845–4854 (2017).
39. Zhang, W. B., Yang, X. T., Ma, J. B., Su, Z. M. & Shi, S. L. Regio- and enantioselective C-H cyclization of pyridines with alkenes enabled by a nickel/N-heterocyclic carbene catalysis. *J. Am. Chem. Soc.* **141**, 5628–5634 (2019).
40. Thongpaen, J., Manguin, R. & Basle, O. Chiral N-heterocyclic carbene ligands enable asymmetric C-H bond functionalization. *Angew. Chem. Int. Ed.* **59**, 10242–10251 (2020).
41. Duan, C.-L. et al. Acetic acid-promoted rhodium(III)-catalyzed hydroarylation of terminal alkynes. *Synlett* **30**, 932–938 (2019).
42. Saidi, O. et al. Ruthenium-catalyzed meta sulfonation of 2-phenylpyridines. *J. Am. Chem. Soc.* **133**, 19298–19301 (2011).

Acknowledgements

We thank Y.-G. Zhou (Dalian Institute of Chemical Physics) and Z.-S. Ye (Dalian University of Technology) for helpful discussions and manuscript revisions. Financial support from Dalian Institute of Chemical Physics (grant no. DICPI201902), Dalian Outstanding Young Scientific Talent (grant no. 2020RJ05) and the National Natural Science Foundation of China (grant no. 22071239) is acknowledged.

Author contributions

Q.-A.C. conceived and supervised the project. Q.-A.C. and G.Z. designed the experiments. G.Z., C.-Y.Z., X.-T.M., Y.L., X.-X.Z., H.L., D.-W.J. and Y.-C.H. performed the experiments and analysed the data. All authors discussed the results and commented on the manuscript.

Competing interests

The authors declare no competing interests.

Additional information

Supplementary information The online version contains supplementary material available at https://doi.org/10.1038/s41929-022-00825-z.

Correspondence and requests for materials should be addressed to Qing-An Chen.

Peer review information *Nature Catalysis* thanks Mengchun Ye, Wei Guan and the other, anonymous, reviewer(s) for their contribution to the peer review of this work.

Reprints and permissions information is available at www.nature.com/reprints.

Publisher's note Springer Nature remains neutral with regard to jurisdictional claims in published maps and institutional affiliations.

Springer Nature or its licensor holds exclusive rights to this article under a publishing agreement with the author(s) or other rightsholder(s); author self-archiving of the accepted manuscript version of this article is solely governed by the terms of such publishing agreement and applicable law.

© The Author(s), under exclusive licence to Springer Nature Limited 2022